

Comparison of Surface Texture from Various Surface Morphology Techniques for Evaluating As-Built Ti6Al4V Laser Powder Bed Fusion

Alex De La Cruz¹, Francisco Medina¹, Edel Arrieta¹, Luke Weston², Mark Benedict², Thao
Gibson³

¹ University of Texas El Paso, El Paso, TX

² Air Force Research Laboratory, WPAFB, OH

³ University of Dayton Research Institute, Dayton, OH

Abstract

Additive manufacturing (AM) is capable of creating unique and complex geometries that conventional methods cannot achieve. The applications for AM have been rapidly increasing across a variety of sectors, particularly for biomedical and aerospace components, the relatively low production volumes and high demand for customizability in both sectors are especially amiable to AM. However, without post-processing, AM components contain a variety of flaws, such as surface roughness and porosity, that can partially be mitigated by process parameters like scan speed and laser power. Surface roughness is a flaw present for every as-built AM surface that serves as an array of sites for every mode of material failure to occur. Common surface roughness measurements involve the use of optical and contact stylus profilometry. However, x-ray Computed Tomography (xCT) is already the most widely used method of analyzing AM parts for porosity, inclusions, and various other flaws. In terms of resolution, xCT should be fully capable of analyzing surface roughness and is the only method of the three investigated that can inspect interior geometries. Therefore, evaluating xCT as a fully inclusive analysis method for AM parts is advantageous. In this study, we compared three surface characterization technologies, xCT, optical profilometry, and contact stylus profilometry. The comparison of these technologies is being done on as-built Laser Powder Bed Fusion (L-PBF) Ti6Al4V four-point bending fatigue samples. Further understanding the difference among each of the technologies will aid ongoing research on developing a standard for xCT surface characterization while also providing more knowledge and insight into each technique and what can be expected. Each of the samples was produced by varying scanning speed and laser power, resulting in different surface textures. Preliminary results show deviations of Sa __%, Sz __%, Sv __%, and Sku __% between the xCT and optical microscopy methods are comparable between these two methods.

1. Introduction

Laser Powder Bed Fusion (L-PBF) is an Additive Manufacturing (AM) method that builds a metal component by melting metal powder particles layer by layer via a laser source or electron beam until the desired geometry is completed [1], [2]. This method brings liberty to the

user by manufacturing complex and unique geometries that traditional manufacturing methods cannot obtain. For instance, AM processes are additive in the sense that they add material to create the part design rather than removing material as is the case with subtractive processes such as milling or turning [3]. This emerging technology could be used to produce tools and components at a very high rate for a wide range of industries, including biomedical, aerospace, and automotive [2]. Such materials that are prominent in the industry for their high performance are titanium (Ti6Al4V), 17-4 PH stainless steel, cobalt chrome, and Inconel 625, which have been shown to be suitable materials for AM production [4]. The overall uses of AM components depend on several factors such as their effectiveness, durability, and overall performance. These influences highly depend on their general surface texture and the surface characterization of their defects, which have the potential to alter the performance efficiency and quality of the component by reducing their durability as well as life expectancy [5]. Additionally, the as-built surface texture is a reflection of the L-PBF machine configurations, such as the powder particle size, layer thickness, beam power, incident angle, and build orientation, all of which are determined before the building process [6]. As-built surfaces of AM-produced components tend to have higher surface roughness, which results in more valleys and peaks that act as stress concentration zones, resulting in a less efficient part [5]. The industry is still in need of a standard that can be utilized to consistently quantify and be able to anticipate the performance according to the L-PBF printing parameters as well as surface texture characterization, notwithstanding the difficulty of measuring the surface texture of AM parts [6].

As the surface texture is an essential and valuable measure, a study was performed where a comparison of different and most commonly used optical measuring technologies such as Confocal Microscopy (CM), Coherence Scanning Interferometry (CSI), Focus Variation Microscopy (FVM), Computed X-ray tomography (XCT) was done to compare their discrepancies [4]. Optical technologies offer a non-destructive surface measuring method of the surface area where post-processing of this data is needed to determine surface roughness measurement S_a . In contrast, contact methods such as a profilometer use a probe tip that is placed on the surface of the sample and records a line profile that will measure the sample's roughness measurement, known as R_a [7]. Furthermore, the contact stylus has been widely used for the measurement of roughness and is the main reference instrument where it provides traceable measurements of form and surface texture [6]. CM offers high lateral and axial resolution, which are dependent on the objective magnification and numerical aperture [7]. A CM uses a pinhole disk in which the light from the LED source is focused through the pinhole disk and the objective lens onto the sample surface, which will reflect the light that is being projected [8]. The reflected light will be filtered by the pinhole disk, so only in-focus light reaches the camera sensor [8]. CSI, also known as white light scanning interferometry, is a technique based on far-field optical microscopy that uses white light interference fringes as a probe scanned over the depth of the sample in order to measure the surface roughness [9]. FVM utilizes an optic with a limited depth of field combined with a vertical scanning process where a series of images is

recorded as the optic is moved vertically along the optical axis, resulting in a vertical image stack that later will be condensed and stitched together using a software algorithm to create a 3D image [10]. Moreover, the non-destructive method xCT has gained significant attention by allowing the user to inspect their manufactured AM parts' geometry internally and externally without the need to cut or destroy it [2]. However, some notable factors that affect the reconstruction of the xCT data and measurement are resolution, sample material, and machine features [2]. In addition, another factor that impacts the resolution, as well as the ability to measure the surface effectively, is the magnification and voxel size, which highly contribute to the final resolution of the surface [2]. A method that is used in xCT data analysis is surface determination from the gray value distribution, which allows for the separation of the material from the background using the gray histogram [2]. xCT and the implementation of this technology in the industry are rapidly growing industries in the use of this technology for the characterization of parts and other applications are the manufacturing, electrical, and food industries.

As previously stated, Ra and Sa are two parameters that quantify the surface roughness of a component. However, a clear distinction between both of these measuring parameters is that Sa is a surface area measurement, as opposed to Ra, which is a line profile measurement [2]. Sa, the areal parameter presents more insight into irregular surfaces of AM parts as it takes into account the whole analyzed areal topography not only a line profile [2]. AM manufacturing companies characterize their surfaces using Ra and Rz measurement methods, and little research shows the use of areal measurements and other parameters either with tactile or optical instruments [3]. From Triantaphyllou's study, it was concluded that Sa and Sq measurements were found to be suitable areal measurement parameters for AM surfaces when compared between two AM technologies, EBM and SLM. In this study, we analyzed the surface roughness Ra and Sa values using three different technologies: xCT, Keyence VR 5200, and SURFTEST SJ-210 Profilometer. The measurements were taken after samples were manufactured via an L-PBF machine at varying printing parameters. The chosen samples were later fatigue tested. These technologies are distinctive; however, this research will assist and provide more insight into the use of xCT to determine the surface roughness of AM components in anticipation of progressing and implementing this technology and standardizing this method. The comparison of three different surface measuring technologies is to provide a thorough comparison and quantify the accuracy of measuring surface roughness across different platforms of commonly used technologies. In addition, this study will provide more insight when measuring surface roughness from AM-produced samples not on what technology is the best form of measurement but provide data and results on what technology would be best applicable to the application in hand.

2. Materials and Methods

2.1 Manufacturing of components

Samples that were used in this study were manufactured via the L-PBF EOS M-290 machine with dimensions of 5 mm x 5 mm x 70 mm. The primary material that was used for all samples was Ti6Al4V; however, the material density was not taken into account upon manufacturing to ensure xCT measurements were precise, as material density does have an effect on the X-ray absorption when conducting xCT measurements [2]. The samples were manufactured at varying printing parameters by altering the speed and power of the L-PBF machine laser source, which resulted in regions known as keyhole, process window, and lack of fusion, the power and speed specifications are illustrated on Fig. 1.

Parameter	Power (W)	Speed (mm/s)
Keyhole	370	800
Process Window	370	1400
Lack of Fusion	370	2000
EOS NOM	280	1200
EOS NOM IM	280	1200

Fig 1. Printing parameter power and speed specifications per regime

Keyhole regions are called such due to the deeply penetrating heat-affected zone due to low speed but high-power input, which resembles a keyhole in cross-section. Lack of fusion regions are regions with insufficient heat transfer due to high speed and low power which results in poor melted and fused together layers, this region tends to have rough edges, pores, and trapped powder. Process window regions are regions where mechanically desirable microstructures are produced. The latter case is only possible in the “window” of process parameters that both create fully dense metal by fully and uniformly melting the metal without overheating it. Process window parameters vary between alloy systems and AM machines and are part of the reason AM is difficult to qualify in actual applications. In addition, we printed samples with EOS standard printing parameters, which resulted in two additional parameters being formed that are also within the process window regime. In this study, the two additional parameters from EOS standards will be labeled as EOS nominal (EOS NOM) and EOS nominal improved (EOS NOM IM). A total of five parameters were used and modifying and altering the power and speed of the laser will allow us to achieve different surface finishes on the as-built surfaces of the components [7], [11]. Furthermore, stress leaving was a post-process applied to each print to reduce the effect of internal thermal stresses after the manufacturing process. The stress-relieving temperature was set at 600°C for 120 minutes with a heating and cooling rate of 5°C/min.

2.1 X-Ray Computed Tomography

The xCT measurements were conducted using a ZEISS Xradia 620, where two voxel resolutions were used per sample, one at a 3.5 μm voxel resolution with a 0.4x magnification and the other at a 0.7 μm voxel resolution at a 4x magnification. The high voxel resolution (0.7 μm) was taken at an area of 1 mm x 1 mm where the larger voxel resolution (3.5 μm) was capable of capturing the samples four faces. For both of the voxel resolutions, the power and voltage remained consistent at 140 kV and 21 W. The 3.5 μm voxel resolution xCT machine parameters were set to the following: sample field of view of 7.4 mm², detector distance to sample of 210 mm, source distance to a sample of 25 mm, exposure time of 4.5 sec per projection, and the source filter set at HE1. While the 0.7 μm voxel resolution samples were scanned with a sample field of view of 1.4 mm², a detector distance to the sample of 77 mm, a source distance to the sample of 20 mm, an exposure time of 20 seconds per projection, and the source filter set to HE3. The source filters were chosen according to ZEISS guidelines and were determined based on the response to the transmission of the sample at 140 kV/21W. The functions of the filter are used primarily for improving the reconstruction of the image quality by removing low-energy X-rays that passed through the sample [13].

Upon completion of xCT, all datasets of each sample were analyzed using VGSTUDIO Max software from Volume Graphics. The procedure taken upon importing dataset files in VG-Studio Max was followed by altering the grayscale histogram and separating our material component from the background and excessive noise. We added a clipping-box tool, where the dataset was clipped to a designated area avoiding any excess material bleed causing inaccurate results when conducting surface analysis measurements. The clipped box was then converted into a Region of Interest (ROI), where a new volume was created by extracting the ROI. An advanced surface-determination tool was incorporated into the model to properly separate the material and excess noise that was left behind due to the grayscale histogram, it has been also shown that the “integrated surface determination” setting shows a much better separation of material and background noise. [AR 4.13 on how the integrated surface determination is better]. We then converted the extracted modified surface to an STL file using high simplification to reduce the amount of computing power. The STL file was then imported into the Omnisurf surface analysis software from Digital Metrology. This method was useful for both voxel sizes of 0.7 μm and 3.5 μm ; however, the 3.5 μm voxel resolution dataset contained all four sides of the component whereas the 0.7 μm voxels were taken at an area of 1 mm x 1 mm. We followed the same procedure previously described and created an STL surface mesh for the 3.5 μm voxel resolution samples on the loading and supporting pin sides for the fatigue testing.

The STL meshes were then imported into Omnisurf software which has the capability to analyze xCT surface meshes and output surface roughness (Sa) and line profile roughness (Ra) values. Upon adding the surface mesh, we re-cropped the STL mesh to a 750 μm x 750 μm area, this was done to ensure comparability with high voxel resolution scans which were at a 1 mm x 1 mm area with low voxel resolution as well as with Keyence measurements. After the cropping is

done, we then ensure to use a bi-cubic fill which results in filling in any missing data the STL might be missing due to the exportation of the STL mesh. Gaussian S and L filters were also applied following ISO standard 25178-3 where an S-filter of 0.0025 mm and an L-filter of 2.5 mm resulted in a bandwidth ratio of 1000:1.

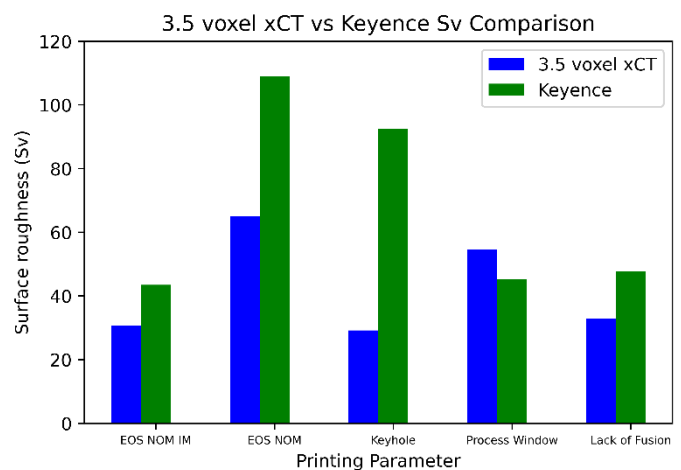
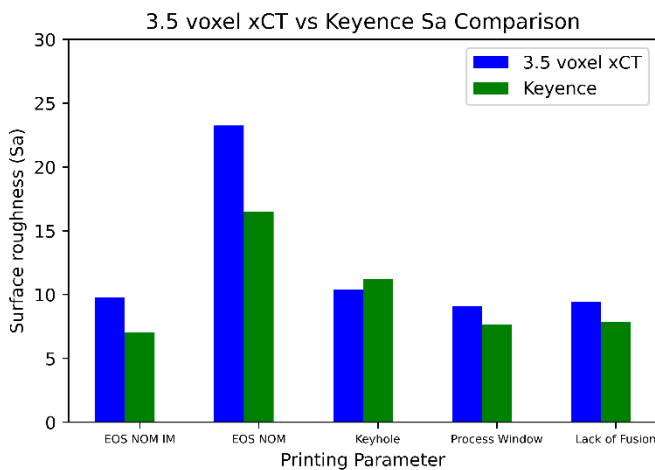
2.3 Profilometer

A Surftest SJ-210 Mitutoyo surface roughness measuring tester was used in the analysis of each sample where the roughness value (Ra) was measured. The specifics of the SJ-210 profilometer are as follows: a tip diameter of 5 μm , a cut-off filter of 0.8 mm, a transversal speed of 0.5 mm/s, with a total of 5x sampling lengths following ISO 4287 (1997) standard which was selected within the device's software.

2.4 Keyence

The Keyence VR 5200 was used to measure both Sa and Ra values from each sample, where the magnification were taken, at 80x, and the measurements were taken on the tension and compression sides, on which the supporting and loading pins made contact during the four-point bend test, respectively. The measurements were taken at three different locations in each parameter sample, and the average values are reported. A key factor when using the Keyence is the S-filter needs to be determined. The S-filter is an aerial gaussian filter used to create cutoffs for sampling distance and sphere radius according to ISO 25178-3 [12]. These cutoffs were important in surface roughness analysis because the L-PBF samples were as-built surfaces, and some un-melted particles were observed on the surface visually as well as optically. Thus, a 50 μm S-filter was selected to measure only the roughness of the sample surface, rather than particles stuck to the sample. The Keyence was used for both Sa and Ra measurements for all samples where the Sa was taken in a selected area of 750 μm x 750 μm and the profile measurement was taken perpendicular to the build direction with a distance of 750 μm .

3. Results



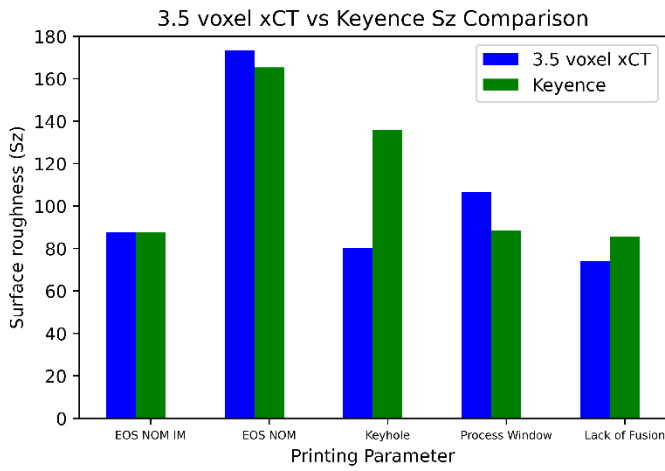


Fig 4: **Sz** Comparison on 3.5 voxel xCT vs Keyence

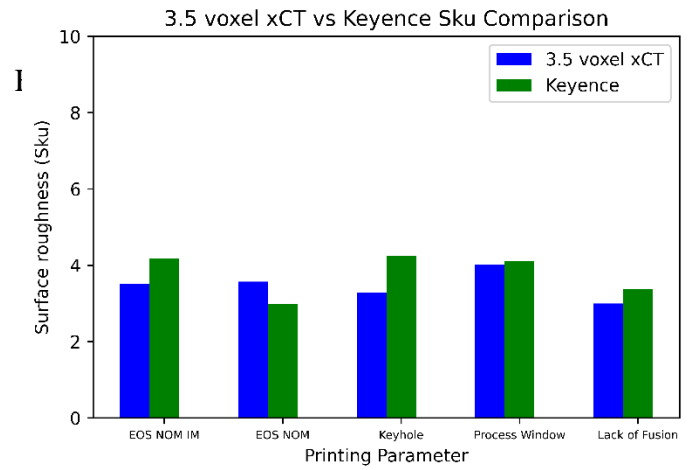


Fig 5: **Sku** Comparison on 3.5 voxel xCT vs Keyence

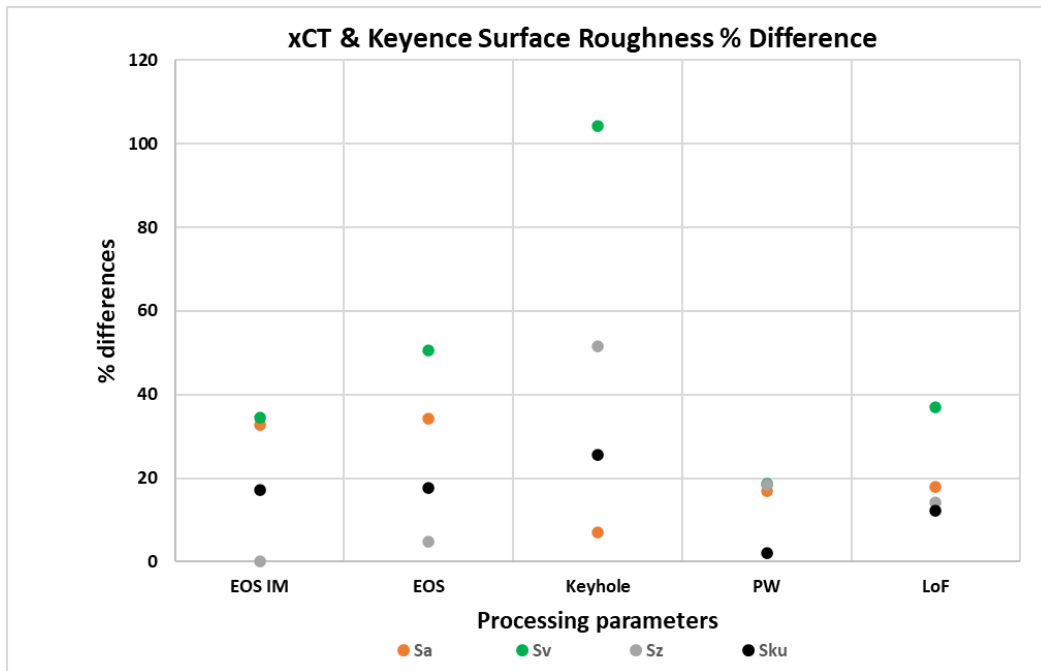


Fig 6: Graphical representation of % different among xCT vs Keyence Surface roughness values (Sa, Sz, Sv, Sku)

% Sa Difference	
EOS NOM IM	32.69 %
EOS NOM	34.17 %
Keyhole	7.35 %
Process Window	17.04 %
Lack of Fusion	17.99 %

% Sv Difference	
EOS NOM IM	34.47 %
EOS NOM	50.53 %
Keyhole	104.26 %
Process Window	18.71 %
Lack of Fusion	36.93 %

% Sz Difference	
EOS NOM IM	0.03 %
EOS NOM	4.71 %
Keyhole	51.52 %
Process Window	18.30 %
Lack of Fusion	14.14 %

% Sku Difference	
EOS NOM IM	17.11 %
EOS NOM	17.72 %
Keyhole	25.51 %
Process Window	2.12 %
Lack of Fusion	12.10 %

Fig 7: Percentage difference between 3.5 μm voxel xCT vs Keyence per each printed parameter set.

4. Discussion

As previously mentioned, the study was done to compare xCT, optical microscopy and profilometer. While the data only show xCT at a 3.5 μm voxel resolution and Keyence optical microscopy comparison, current and ongoing work is being done to further compare all methods. Further investigation of the study will allow us to aid current research to progress the standardization of xCT method for external and internal measurements. In addition, provide more insight on each technology and their differences when evaluating surface roughness. Moreover, preliminary results show comparable data from xCT 3.5 μm voxel resolution with Keyence optical microscopy.

Fig 2 – Fig 5 is a graphical comparison of parameters, Sa, Sv, Sz, and Sku. Where Sa is the difference in height of each point compared to the arithmetical mean of the surface, Sv is the absolute value of the height of the largest pit, Sz is the sum of the largest peak height value and the largest pit depth, Sku is the sharpness of the roughness also known as Kurtosis. These evaluated parameters are measured within the respected surface area in which is being analyzed which in this case was a 750 μm x 750 μm area. Additionally, Fig 6 illustrates the difference in percentage between the two measuring methods. Where Sv shows the highest differences up to 104.26% for the Keyhole parameter. A current assumption for such a significant difference is the Keyence uses an LED source where it can penetrate in a larger depth to where it can obtain the valley depth due to the keyhole effect. Whereas xCT may not measure the valley depth or any keyhole effect given that the xCT mesh may not be capable of exporting every deeply penetrated

regions due to the keyhole parameter set. Sa shows a comparison where the highest difference is 34.17% for the EOS NOM parameter, respectively, where this parameter lies within the process window regime. For both Sku and Sz differences showed a comparison where the highest was 51.52% for Sku and 25.51% for the Keyhole parameter, respectively. Fig 7 shows each surface roughness value percentage difference between each surface roughness and printed parameter.

5. Conclusion

In conclusion, the results that were displayed are partial and ongoing research is being done to further compare all technologies cohesively to further compare surface roughness as well as line profile roughness. While previous research has noted that surface roughness parameters such as average roughness (Sa or Ra) mean roughness depth (Sz or Rz), skewness (Ssk or Rsk) and kurtosis (Sku or Rku) could be used for the characterization of additive manufactured parts [4]. Our study and choosing of surface roughness parameters was done for the evaluation of fatigue tested samples where Sv could give us more insight into fatigue life and better understanding in the correlation of surface roughness and fatigue life. However, the correlation between fatigue life and surface roughness was not taken into consideration in this study.

Current Sa, Sv, Sz, and Sku results do show a good comparison considering each printing parameter where Sa showed the highest difference of 34.17%, Sv showed the highest of differences up to 104.26 %, Sz highest difference of 51.52%, and Sku highest difference of 25.51%. Amongst the measured values, Sv showed the least comparable given the highest difference of 104.26% and the lowest difference of 18.71%. The reason for this is still unknown and with further comparisons, and a more thorough literature review, we strive to reach a conclusion and understanding. Additional investigation will be done to have more insight and understanding why the keyhole regime had the highest values of Sv, Sz, and Sku. Factors that could affect these parameters can include but are not limited to scanning strategy, number of contours, as well as placement on the plate, where these factors were not taken into consideration in this study. Moreover, this study was not done to conclude what technology is best or more convenient but to give a better understanding of when to use a given technology for a certain and given application. For example, xCT will be of great use when the component being analyzed needs thorough internal and external investigation, given that xCT has the capability to internally and externally characterize a component that optical and profilometer methods cannot achieve. Also standardizing xCT methods and having repeatability amongst surface roughness results will give the capability to implement this form of surface measuring method to complex geometries for industrial applications. Future research could be to compare these technologies and their surface roughness results for the qualification of manufactured parts. Doing so will give a representation of how these technologies could be used for the inspection and qualification of surface roughness for industry and research.

6. References

- [1] R. K. Leach, D. Bourell, S. Carmignato, A. Donmez, N. Senin, and W. Dewulf, “Geometrical metrology for metal additive manufacturing,” *CIRP Ann.*, vol. 68, no. 2, pp. 677–700, 2019, doi: 10.1016/j.cirp.2019.05.004.
- [2] C. Sen, G. Dursun, A. Orhangul, and G. Akbulut, “Assessment of Additive Manufacturing Surfaces Using X-ray Computed Tomography,” *Procedia CIRP*, vol. 108, pp. 501–506, 2022, doi: 10.1016/j.procir.2022.03.078.
- [3] A. Triantaphyllou *et al.*, “Surface texture measurement for additive manufacturing,” *Surf. Topogr. Metrol. Prop.*, vol. 3, no. 2, p. 024002, May 2015, doi: 10.1088/2051-672X/3/2/024002.
- [4] A. Townsend, N. Senin, L. Blunt, R. K. Leach, and J. S. Taylor, “Surface texture metrology for metal additive manufacturing: a review,” *Precis. Eng.*, vol. 46, pp. 34–47, Oct. 2016, doi: 10.1016/j.precisioneng.2016.06.001.
- [5] L. Ednie *et al.*, “The effects of surface finish on the fatigue performance of electron beam melted Ti–6Al–4V,” *Mater. Sci. Eng. A*, vol. 857, p. 144050, Nov. 2022, doi: 10.1016/j.msea.2022.144050.
- [6] W. Sun *et al.*, “Establishment of X-ray computed tomography traceability for additively manufactured surface texture evaluation,” *Addit. Manuf.*, vol. 50, p. 102558, Feb. 2022, doi: 10.1016/j.addma.2021.102558.
- [7] M. Heintl *et al.*, “Measuring procedures for surface evaluation of additively manufactured powder bed-based polymer and metal parts,” *Meas. Sci. Technol.*, vol. 31, no. 9, p. 095202, Sep. 2020, doi: 10.1088/1361-6501/ab89e2.
- [8] T. Grimm, G. Wiora, and G. Witt, “Characterization of typical surface effects in additive manufacturing with confocal microscopy,” *Surf. Topogr. Metrol. Prop.*, vol. 3, no. 1, p. 014001, Jan. 2015, doi: 10.1088/2051-672X/3/1/014001.
- [9] K. L. Apedo *et al.*, “Cement paste surface roughness analysis using coherence scanning interferometry and confocal microscopy,” *Mater. Charact.*, vol. 100, pp. 108–119, Feb. 2015, doi: 10.1016/j.matchar.2014.11.033.
- [10] L. Newton *et al.*, “Areal topography measurement of metal additive surfaces using focus variation microscopy,” *Addit. Manuf.*, vol. 25, pp. 365–389, Jan. 2019, doi: 10.1016/j.addma.2018.11.013.
- [11] J. Delgado, J. Ciurana, and C. A. Rodríguez, “Influence of process parameters on part quality and mechanical properties for DMLS and SLM with iron-based materials,” *Int. J. Adv. Manuf. Technol.*, vol. 60, no. 5–8, pp. 601–610, May 2012, doi: 10.1007/s00170-011-3643-5.
- [12] International Organization for Standardization. 2012. “ISO Standard 25178-3 1st ed., Ser. Geometrical product specifications (GPS): Surface texture: Areal.”
- [13] Carl Zeiss X-ray Microscopy, Inc. 2019. “Xradia Versa 3D X-ray Microscope User Guide”